ADVANCED FUNCTIONAL MATERIALS
www.afm-journal.de

Highly Desirable Photodetectors Derived from Versatile Plasmonic Nanostructures

*Hongyu Chen, Longxing Su, Mingming Jiang, and Xiaosheng Fang**

With unique ability to concentrate and manipulate light at nanoscale, surface plasmon resonance technologies create additional opportunities for fabricating superintegration photodetectors with desirable functionalities. To gain an insight into the state-of-the-art of plasmonic photodetectors, recent advances in novel devices as well as potential building blocks are presented herein. The article focuses particularly on understanding the enhancement mechanism of different architectures such as nanoparticles, gratings, waveguides, antennas, and microcavities. Meanwhile, challenges and potential design schemes are proposed in this inspiring field.

1. Introduction

As a momentous component of information technology (IT), photoelectric sensor technology has attracted considerable attention owing to its tremendous application potentials in many domains with regard to industry, agriculture, environment and medical care. In particular, cooperated with communication technology and computer technology, versatile photoelectrical sensors provide us great abilities to understand and change the world.[1–4] For example, thanks to the visible and infrared (IR) sensors on a meteorological satellite, one can update the actual weather whenever and wherever possible; owing to the IR night vision, drivers could see much better on dark road; and ultraviolet (UV) sensors play an important role in monitoring ozone hole,[5] air/water purifcation and so forth; moreover, the high resolution imaging sensors in the endoscope of da vinci surgical system not only bring faster and more accurate clinical diagnosis by 3D view of inside the internal organ, but also make the surgical therapy more convenient and effective, etc.[6] Therefore, further research and development of photoelectrical sensor technology will be of great significant both in human health and social progress.

Generally, in the photoelectrical sensor system, a photodetector offers the ability to convert light into electrical signals, whose performance and architecture will directly affect the design of post-stage readout and amplifying circuits. Hence, it is no doubt that making a future roadmap of photodetector is still at the heart of developing next generation photoelectrical sensor technology. At the same time, to make the integrated photoelectric conversion system operate with desirable performance, the size of photodetector should be small enough which is compatible with the constantly developing superintegrated circuits. As shown in **Figure 1**a, it is the evolution of metal-oxide-semiconductor field-effect transistor gate length in production-stage integrated circuits in conjunction with international technology roadmap for semiconductors (ITRS) targets figured in 2010.[7] It is not hard to find that the gate lengths of the transistor exponentially decreased as time went on. Correspondingly, number of transistors per processor chip increased exponentially. And following ITRS target, it is believed that the gate length will be shrunk from 30 to 7.4 nm in ~15 years. However, IBM realized the target at an alarming rate—a decade ahead of ITRS schedule! They announced their successful production of 7 nm test chips at its joint research lab at State University of New York (SUNY) polytechnic institute in 2015 (Figure 1b).[8] It is no doubt that scaling down the size of optoelectronic cell has enabled the complexity of integrated optoelectronic devices with high performance and multifunctionality. However, shrinking down the size of photodetectors along with their post-stage circuits will face tremendous challenges. As an example, to realize high photoelectric conversion efficiency, most active materials in the photodetectors need necessary size for sufficient optical absorption. If the active area of optoelectronic device is decreased, it will result in a degraded sensitivity of ptotodetection. Moreover, when their sizes are reduced down to subwavelength scale, conventional devices will suffer from optical diffraction limit and start to misbehave. Hence, to develop superintegrated photodetectors with high

Dr. H. Y. Chen, Dr. L. X. Su, Prof. X. S. Fang
Department of Materials Science
Fudan University
Shanghai 200433, P. R. China
E-mail: xshfang@fudan.edu.cn
Dr. H. Y. Chen
Department of Physics
Harbin Institute of Technology
Harbin 150001, P. R. China
Dr. H. Y. Chen
Key Laboratory of Micro-systems and Micro-structures
Manufacturing of Ministry of Education
Harbin Institute of Technology
Harbin 150080, P. R. China
Prof. M. M. Jiang
State Key Laboratory of Luminescence and Applications
Changchun Institute of Optics
Fine Mechanics and Physics
Chinese Academy of Sciences
Changchun 130033, P. R. China
The ORCID identification number(s) for the author(s) of this article can be found under https://doi.org/10.1002/adfm.201704181.

DOI: 10.1002/adfm.201704181

performance, design solutions which could decrease the size of single photodetector and increase its photoelectric conversion efficiency at the same time are emergency needed.

Fortunately, it is delighted to find that plasmonic nanostructures share a unique capability to concentrate, route, and manipulate light at nanoscale. It provides us a promising approach to bridge the gap between the world of nanoscale electronics and microscale photonics.[9,10] And some prominent experimental and technological applications were obtained in sensor, solar cell, light-emitting diode, laser, and so on.[11–13] Especially, experimental results demonstrate that incorporation of plasmonic nanostructures in photodetectors not only has the potential to overcome the problem of light trapping at subwavelength scale, but also could suppress photon-generated carrier recombination.[3] Although many operating mechanisms of present plasmonic photodetectors are not very clear, versatile photodetectors have been designed and fabricated in conjunction with various metallic and graphene nanostructures such as nanoparticle,[14–16] grating,[17–19] waveguide,[20,21] antenna,[22,23] and microcavity,[24–28] etc. These results demonstrated that photodetectors involvement of surface plasmon resonance have great potential to be applied in more domains with higher performance and greater functionality (Figure 1c). Briefly, in addition to enhance the quantum efficiency, signal-to-noise, and bandwidth of photodetectors, properties inherent to surface plasmon resonances are also exploited to provide additional characteristics to photodetectors including polarization, angular, and spectral selectivity, etc.[29–32] Up to now, albeit extensive researches on plasmonic photodetectors were reported, review of plasmonic photodetectors involving potential plasmonic materials and building blocks is still lacking.

Herein, current literatures on photodetectors enhanced by surface plasmon resonance technique are demonstrated systematically in this paper. Briefly, a comprehensive description of photodetection mechanisms in these plasmonic photodetectors is proposed at first, and then a few representative applications of the state-of-the-art plasmonic photodetectors as well as some promising plasmonic building blocks are described before outlining the challenges and opportunities in this exciting area.

2. Operating Mechanisms of Plasmonic Photodetectors

A plasmonic photodetector is a kind of photoelectric device with the capability to detect surface plasmons or involving surface plasmon resonances in their photodetection process.[31] To understand how surface plasmon resonance can be applied for enhancing the performance of photodetectors, it is essential to gain insight into both the nature of surface plasmon resonances and photodetectors at first. Because the design schemes and working mechanisms of various photodetectors have been fairly demonstrated in previous reviews,[4,33,34] they will not be presented here. As such, some basic knowledge of surface plasmon resonances will be briefly outlined, followed by three working mechanism of present plasmonic photodetectors in this section.

Hongyu Chen is a lecturer at the Department of Physics, Harbin Institute of Technology, China. She received her Ph.D. from Changchun Institute of Optics, Fine Mechanics and Physics, Chinese Academy of Sciences, in 2014. Since then, she worked as a postdoctoral fellow in the Department of Materials Science, Fudan University, China. Her current research interests include designing, fabricating, and exploring novel properties of optoelectronic devices based on semiconductor and metallic materials, which have a special focus on low dimensional photodetectors.

Longxing Su received his Ph.D. in condense matter physics from Sun Yat-Sen University, China. After graduation, he joined San'an Optoelectronics Co., Ltd. as a research engineer and focused on the development of blue-light-emitting diodes (LEDs). He is currently a postdoctoral fellow in the Department of Materials Science, Fudan University, China. His current research topic is the fabrication, characterization, and application of II–VI inorganic semiconductor-based photodetectors.

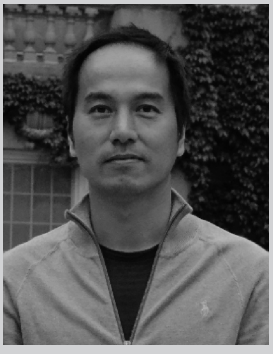

Xiaosheng Fang received his Ph.D. from the Institute of Solid State Physics, the Chinese Academy of Sciences, in 2006. Afterward, he worked as the National Institute for Materials Science (NIMS), Japan as a JSPS postdoctoral fellow, as well as an International Center for Young Scientists (ICYS)-International Center for Materials Nanoarchitectonics (MANA) researcher. Currently, he is a Professor in the Department of Materials Science, Fudan University, China. His research focuses on semiconductor nanostructure-based photodetectors.

2.1. Basic Knowledge of Surface Plasmon Resonances

Surface plasmon is a kind of hybrid electromagnetic wave arising from the collective oscillations of free electron gas within the metal, which could propagate along the interface between a metal and a dielectric (**Figure 2**a).[35] With the unique ability to route

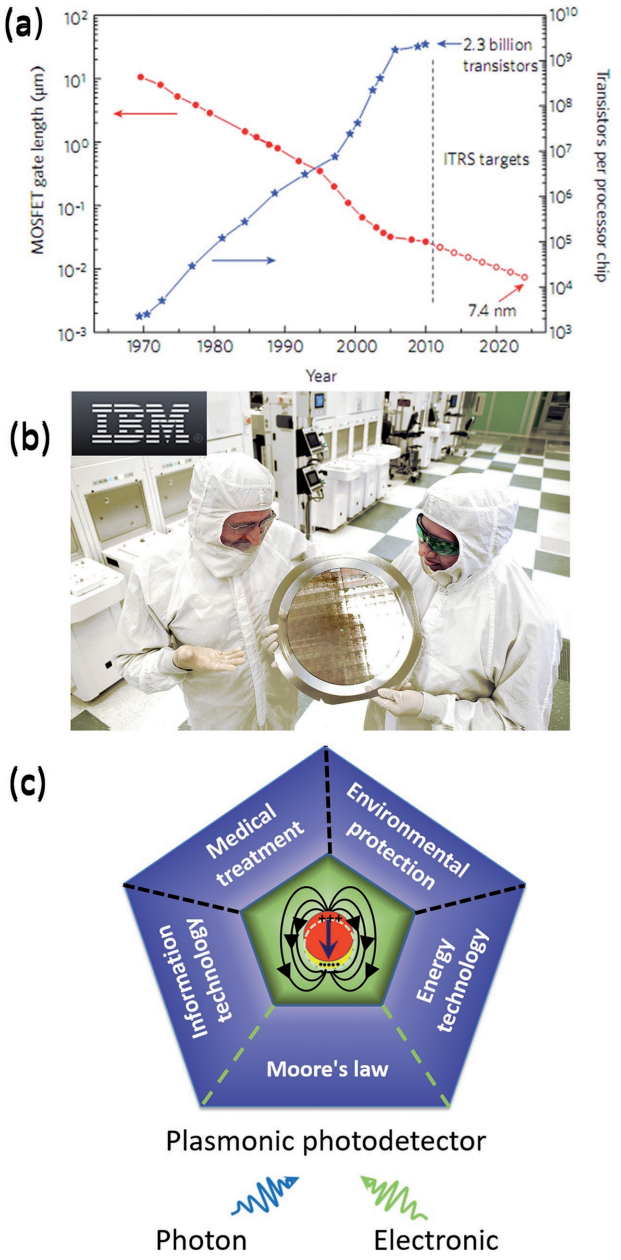

Figure 1. a) Trends in digital electronics figured at 2010. Evolution of MOSFET gate length in production-stage integrated circuits and ITRS targets. Reproduced with permission.[7] Copyright 2010, Macmillan Publishers. b) IBM announced their successful production of 7 nm test chips at the SUNY Polytechnic Institute in 2015. Reproduced with permission.[8] c) A roadmap of next-generation photodetectors based on surface plasmon techniques.

and manipulate light at nanoscale beyond diffraction limit, it has been of significant interest in the development of nanophotonic devices.[36] Nowadays, the family of their associated materials has grown up from insulator throughout semiconductor even zero-band-gap semiconductor (i.e., graphene) to metal, which is an important component of fascinating nanophotonics. However, surface plasmons were not considered viable for photonic elements for a long time because of the significant propagation losses arising from the metal absorption. Thankfully, further researches demonstrated that surface plasmons components are significantly smaller than the propagation length.[37] These important discoveries open the way to integrate surface plasmons components into photoelectronic devices with low losses. In addition, the excitation and propagation of a suitable surface plasmon resonance mode at the desirable wavelength need the ability to control a complex condition consisting of plasmonic nanostructures' shape, size, composition, as well as their dielectric environment. Therefore, to design and fabricate plasmonic photodetectors with desirable performance, integration of an appropriate surface plasmon mode is of paramount importance.

According to the propagation length of surface plasmons, the mode of surface plasmon can be classified into two main categories: localized surface plasmons (LSPs) and surface plasmon polaritons (SPPs). As illustrated in Figure 2b, LSPs are non-propagating excitations of the conduction electrons of metallic nanostructures which could be coupled to the electromagnetic field. The resonance frequency and bandwidth of this mode is mainly determined by the metallic nanostructure's shape, size, and environment. Generally speaking, small particles such as islands, spheres, and rods supported LSPs, and the phenomena of light trapping or scattering by small particles have a long and interesting history in physics and materials. Fabricating high performance photodetectors within random or regular morphology of metallic nanostructures have been reported for a long time, specific description of this type devices will be proposed later in Section 3.1.1. By contrast with LSPs, SPPs could propagate along the interface between a metal and a dielectric. As such, they are also known as propagating surface plasmons. They can be supported on a variety of metal–dielectric structures including metal nanoparticles,[14–16] hybrid plasmonic waveguide consisting of metal and dielectric films,[20,38] metal gratings,[17–19] antennas,[22,39] and microcavties.[25–27] Similar to LSPs, SPPs are sensitive to the surrounding environment in the vicinity of metal/dielectric interface. It is also worth pointing out that the excitation of SPPs is beneficial to compensate missing momentum, which would be very conducive to guide and trap light into the active layer of photodetectors.

Albeit multifarious plasmonic photodetectors are explored, relationship between the performance of photodetectors and the nature of the surface plasmon modes are still need to be further categorized and clarified. Hence, summary of their operating mechanisms is vital for the further development of this type of devices. In the following paragraph, three main working principles of photodetection enhanced by LSPs and SPPs will be sketched at first, then applications of surface plasmon in photodetectors will be deferred to Section 3.

2.2. Working Principle of Photodetection Enhanced by Surface Plasmons

Generally, detecting optical signals via a semiconductor photodetector is mainly through three-step photoelectric conversion processes: (1) carriers generation by incident light; (2) carriers transportation (as well as carriers multiplication if current-gain mechanism is present); (3) carriers extraction as the output electric signal.[40] Therefore, to fulfill the increasing demand

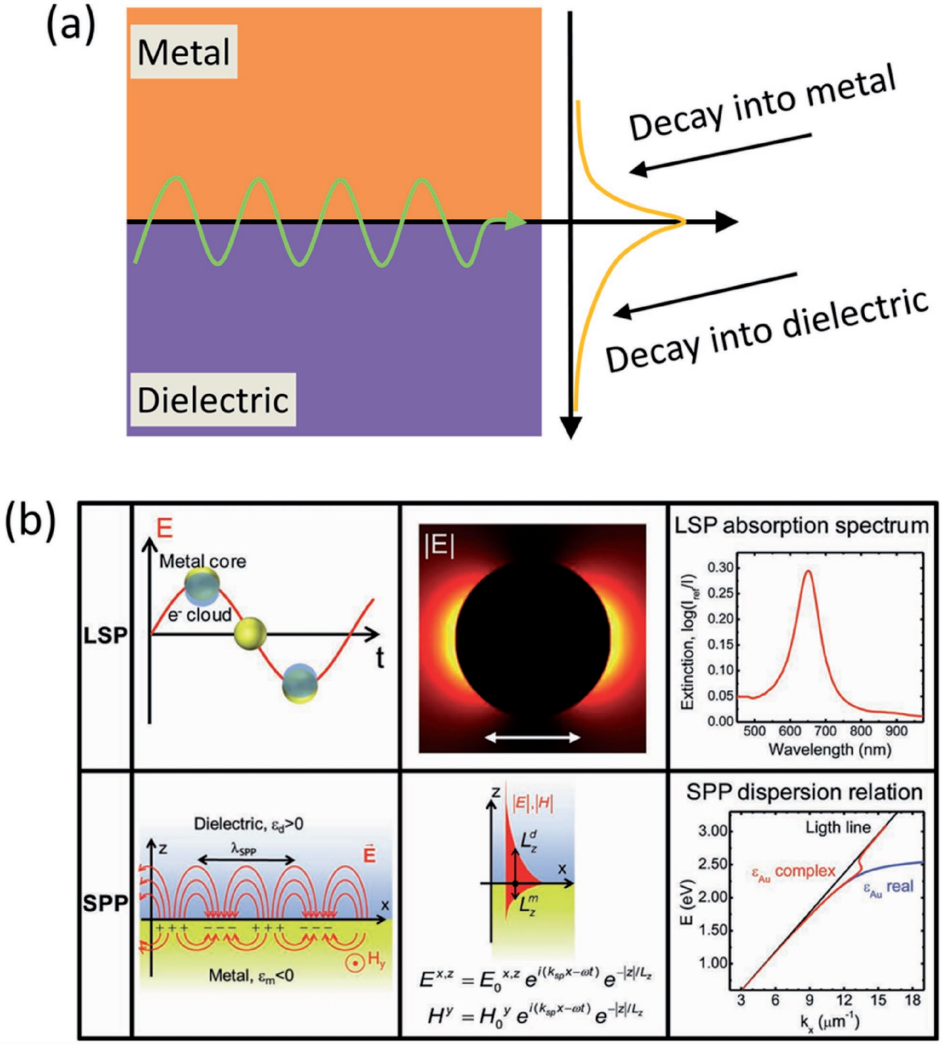

Figure 2. a) Decay length of surface plasmon into metal and dielectric. b) Classification of the surface plasmon polarizations. Reproduced with permission.[35] Copyright 2013, Wiley-VCH.

of high-speed and sensitive photodetectors, fabricating novel photodetectors by using the flourishing surface plasmon technologies, systematically studies these photoelectric conversion processes are vital. Hence, we will lift the veil on the remarkable advantages of plasmonic photodetectors vividly starting from this perspective.[2,3,29,41] First, in the process of carriers generation by incident light, thanks to the increased resonance absorption without consideration of optical diffraction limit, it shrinks the physical dimension of photodetectors without changing optical dimension. And then, in the process of carrier transportation, the resonating electromagnetic fields are significantly enhanced compared to the illuminating fields. The enhanced electromagnetic field surrounding the plasmonic nanostructures may accelerate the separation of electron–hole pairs in the active layer. Furthermore, a lower device capacitance is benefit for obtaining a fast carriers transition time, which is promising to realize high-speed detection. At last, in the process of carrier extraction, the enhanced electromagnetic field would reduce the operation energy for generating electrical signals.

In addition to aforementioned promising results of surface plasmon resonance technique used in conventional photodetectors (**Figure 3**a), an emerging surface plasmons technique enable to detect photons with energies lower than the interband threshold of the semiconductor via generating hot carriers. The underlying physical principle is presented in Figure 3b, c. In these two configurations, resonant surface plasmons can decay either radiatively or nonradiatively through the generation of excited carriers, typically referred to as hot carriers.[42–44] After this type of surface plasmon resonance is photoexcited, additional carrier–carrier scattering and relaxation of the high-energy carriers would generate photocurrent which is no longer limited to the bandgap of semiconductor, but rather extended to Schottky barrier height or tunnel junction. Therefore, these new discoveries would break the limits of semiconductors' bandgap for exploring new photodetectors. Moreover, it will provide a novel approach to modulate the junction and inject more photon-generated carriers for output current, even without bias voltage. As such, owing to plasmon excitations are most taken placed in metallic nanostructures, hybrid system of

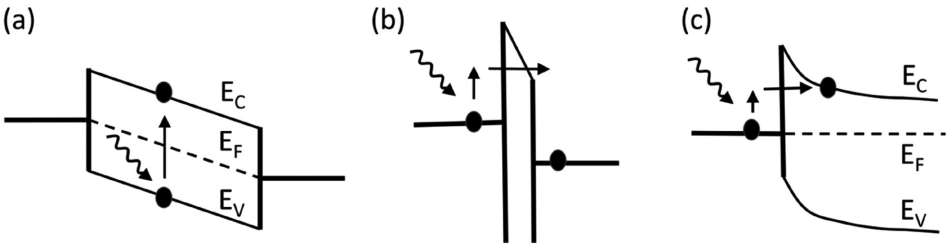

Figure 3. Plasmon detection mechanisms of a) standard semiconductor photodetectors, b) tunnel junction detectors, and c) Schottky diode photodetectors. Reproduced with permission.[44] Copyright 2013, Wiley.

metal–semiconductor would be an excellent building block for manipulating the emission of hot carriers, as well as a promising platform for fabricating plasmonic photodetectors with dual-function.

3. Excitation of Surface Plasmon Resonance in Photodetectors

Through above descriptions, quite a few potential advantages of the surface plasmon resonance technique for the further development of next generation photodetectors have been witnessed, and it is believed that the progression of plasmonic photodetectors would be toward smaller, faster, and more efficient in near future. However, both of LSP and SPP modes are difficult to be efficiently excited, which bring about many challenges in designing and fabricating this kind of devices. For this reason, exploring an effective method that can remarkably harness surface plasmon excitations is particularly critical at present. In this section, existing methods for exciting the surface plasmon resonances in terms of single LSP modes, SPP modes, and coexistence of two modes in the photodetectors will be described in detail. We hope these available technologies may offer some new opportunities for exploring next generation plasmonic photodetectors.

3.1. Photodetectors Enhanced by Single Surface Plasmon Mode

To better stimulate surface plasmon polaritons and achieve their better applications in photodetection, various plasmonic nanostructures have been explored, which attracted many interests in past few years. Under the impetus of rapidly developed chemical synthesis techniques and physical micro–nano fabrication technologies, versatile metallic nanostructures such as rods,[45,46] shells,[47,48] rings,[21,49] rings/disks,[50,51] cubes,[52,53] array of subwavelength slits,[54,55] or holes[56,57] in metal films, etc. as well as graphene[58,59] are fabricated successfully. With different plasmonic characteristic and functions, they played an important role in enhancing the performance of photodetectors. In order to explain the profound physical mechanisms behind these different structure devices in a simple way, background knowledge of surface plasmon modes (LSPs and SPPs) with the typical examples will be demonstrated firstly.

3.1.1. Photodetectors Enhanced by LSP Excitation in Metallic Nanoparticles

As mentioned above (Section 2.1), LSPs cannot propagate freely, they are usually confined in the vicinity of metallic nanoparticles, where the excited electromagnetic field is strongly enhanced compared with the incident optical field. For this reason, incorporation of LSP technique in photodetectors may be a promising pathway to enhance quantum efficiency by additional light trapping and resonance field enhancement, and this has been confirmed by many experimental results.[14–16,60–62] Therefore, with the purpose of taking full use of metallic nanoparticles in plasmonic photodetectors, getting insight into the principle of launching surface plasmons from metallic nanoparticles seems particularly important. As illustrated in **Figure 4**, these modes arise naturally from the scattering effect

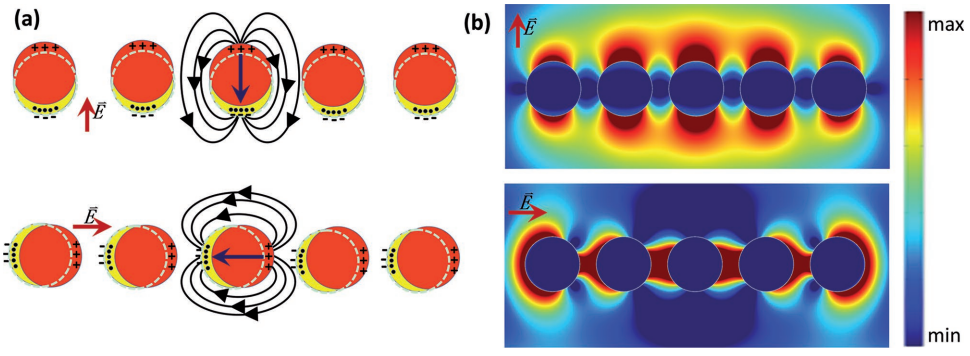

Figure 4. Sketch of a) charge distributions and b) corresponding electric field distributions of the metallic nanoparticles for the two different polarizations.

of a small, subwavelength conductive nanoparticle in an oscillating electromagnetic field.[36] When LSPs generated, electrons (take the simplest spherical particles as an example) would oscillate coherently with the incident light field. If the dimension of particles is compared to the wavelength of incident light, the fundamental resonant mode of these particles is mainly dipolar charge distribution at the surface. These resonant features could be characterized by their extinction (scattering and absorption) spectra. In theory, the experimental results outlined above exhibit a reasonably good approximation with Mie theory for small spherical and ellipsoidal particles in visible and near-infrared region. Generally speaking, in the condition of quasi-static limit ($r \gg \lambda : r$ is the radius of the nanosphere, λ is the wavelength of incident light), the extinction cross-section C_{ext} can be calculated from Equation (1)

$$C_{ext} = C_{sca} + C_{abs} \tag{1}$$

where C_{abs} and C_{sca} are the absorption and scattering cross-sections of the small metallic nanosphere, respectively

$$C_{abs} = \frac{2\pi}{\lambda_0} \mathrm{Im}\{\alpha\} \tag{2}$$

$$C_{sca} = \frac{1}{6\pi}\left(\frac{2\pi}{\lambda_0}\right)^4 |\alpha|^2 \tag{3}$$

and α is the sphere's polarizability, given by the following expression for the case of dipolar resonant mode

$$\alpha = 4\pi r^3 \left(\frac{\varepsilon_m - \varepsilon_d}{\varepsilon_m + 2\varepsilon_d}\right) \tag{4}$$

In Equation (4), ε_m, ε_d, and r are the permittivities of the metal and surrounding dielectric, the radius of the nanosphere, respectively. From the above formulas, it would be easy to conclude that absorption dominates a main component of extinction in the case of a small sphere (the size of the metallic particle is much smaller than the wavelength of incident light), and they absorb energy mainly through three following mechanisms:[63] (i) collective excitations of "free" electrons by surface plasmon resonances, (ii) interband transitions, and (iii) surface dispersion or scattering of "free'' electrons if their mean free path (**Table 1**) is comparable to the dimension of nanoparticles. When the size of nanoparticles increases, the radiation effects become more and more important, which dominate a main component of extinction. If the dimension of particles is larger than their mean free path, higher order resonant modes will appear and the quasi-static approximation will break down due to retardation effects.[64] Owing to the complexity of multipolar surface plasmon induced by controlling the size, structure, and coupling interaction (e.g., Fano interference) of nanoparticles, photodetectors enhanced by multipolar surface plasmons are scarce until now, and it is not be discussed herein.

Table 1. Values of the electron–electron mean free path. The data is reproduced from ref. [65].

Materials	L [nm]	l_p [nm]	l_e [nm]	$l_{e,t}$ [nm]
Au (electrons)	74	≤50	>200	40.6
Au (holes)	55	≤50	>200	52
Ag (electrons)	44	$10 \le l_p \le 60$	$70 \le l_e \le 750$	57
Cu (electrons)	$5 < L < 20$	$10 \le l_p \le 80$	≤ 25	42.1
Pd (electrons)	17	$10 \le l_p \le 80$	$15 \le l_e \le 40$	11

Therefore, present plasmonic photodetectors with metallic nanoparticles may operate as following: owing to metallic nanoparticles, optical energy is scattered by one nanoparticle, and collected by its neighboring one as plasmons instead of decaying as free-space light. In this way, incident light is trapped and localized in the plane of nanoparticle array, and then create additional electron–hole pairs in the semiconductor. Additionally, the improved localized optical field would accelerate the separation of electron–hole pairs, therefore lead to a great enhancement of optical field and photocurrent.

Based on aforementioned working mechanisms, photodetectors enhanced by LSPs were realized by simple random dispersed metallic nanoparticles deposited onto the surface of devices.[66–70] Furthermore, it is found that in addition to the size of the nanoparticles, special morphology such as trilateral, cube nanoparticles would also play an important role in the redistribution of metallic nanoparticles' surface charges for determining the resonance wavelength of the surface plasmons.[15,71–75] As an example, **Figure 5**a is a Se microtube photodetector with a broadband responsivity enhancement from 300 to 700 nm by tailored the sputtering time of disperse Au nanoparticles.[14] And the following theoretical simulations and analyses demonstrate that the intensity of surface plasmon resonance is mainly attributed to the interaction between Au nanoparticles and Se microtube. It is believed that this work would provide us an additional opportunity for fabricating surface plasmon enhanced broadband photodetectors with high-performance. As illustrated in Figure 5b, it is a AlGaN-based plasmonic photodetector with strongest field enhancement by the sharp tips of Al nanoparticle.[15] The peak responsivity of the device is enhanced more than 25 times than that of without size-controlled and well-ordered Al nanoparticles, which offers us a low-cost and high efficient approach to achieve plasmonic enhanced deep UV optoelectronic devices with excellent performance.

3.1.2. Photodetectors Enhanced by Propagating Surface Plasmons

Albeit LSP technique is a convenient way to enhance the optical absorption of semiconductors and photocurrent of photodetectors, an important issue for such devices should be considered, LSP field would attenuate rapidly owing to high loss in the metal.[36] Hence, to compensate the missing momentum, and guide, trap light into the active layer of photodetectors with high efficient, the abilities to convert incident light into a propagating SPP mode, and incorporate such plasmonic circuits into photodetectors are of important. As illustrated in **Figure 6**a, albeit constructing the structure supporting propagating surface plasmons is not difficult, and the simplest way is to build an optical semi-infinite dielectric/metal

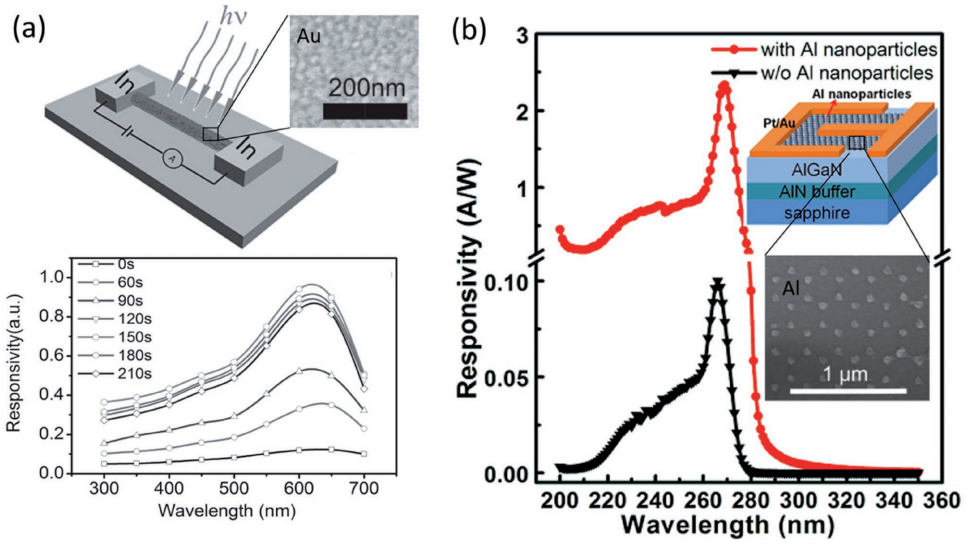

Figure 5. a) Scheme illustration of Se–MT photodetector enhanced by randomly distributed Au nanoparticles (top). Spectral responsivity of single Se–MT photodetectors with various Au sputtering times (bottom). Reproduced with permission.[14] Copyright 2016, Wiley-VCH. b) Spectral response of AlGaN-based metal–semiconductor–metal (MSM) detectors with and without size-controlled and well-ordered Al nanoparticle arrays. Reproduced with permission.[15] Copyright 2015, AIP Publishing.

interface.[36] The propagation of transverse electromagnetic waves is forbidden inside the metal when ω is smaller than ω_{sp} (Figure 6b). Therefore, it is an important challenge for surface plasmons to be launched directly on a smooth metal surface, because β_{SP} (the propagation constant of surface plasmon) of the SPP is greater than that of a free-space photon at the same frequency. To figure out this intractable issue, approaches in terms of prism coupling, a periodic corrugation in the metallic surface such as gate, and waveguide for coupling between light and SPPs are well performed in several coupling photodetectors in order to compensate the missing momentum.

To enhance the momentum of incident light, prism coupling for optical excitation of SPPs by using Kretschmann and Otto configurations are the first two frequent methods for constructing SPPs based photodetectors.[76] By introducing into the totally reflected system, the incident light could be totally reflected at the base of prism when it passes through a high refractive index prism. What is more, the in-plane component of the free-space photon propagation constant k_x ($k_x = k\sin\theta$, θ is the angle to the surface normal) at the metal–air interface is smaller than the SPP propagation constant β, even at grazing incidence, prohibiting phase-matching. This means that SPPs could be excited along the interface with the new propagation constant adjusted by controlling the angle of incidence as following

$$\frac{2\pi}{\lambda} n_p \sin(\theta) = \mathrm{Re}\{\beta_{SP}\} \tag{5}$$

where θ is incidence angle, n_p denotes the refractive index of the prism ($n_p > n_d$), and β_{SP} denotes the propagation constant of the SPPs.

To descript the effect of prism coupling in photodetector vividly, a typical device is described below. In these prism coupling photodetectors, Otto coupling is more popular than Kretschmann coupling in experimental work. As sketched

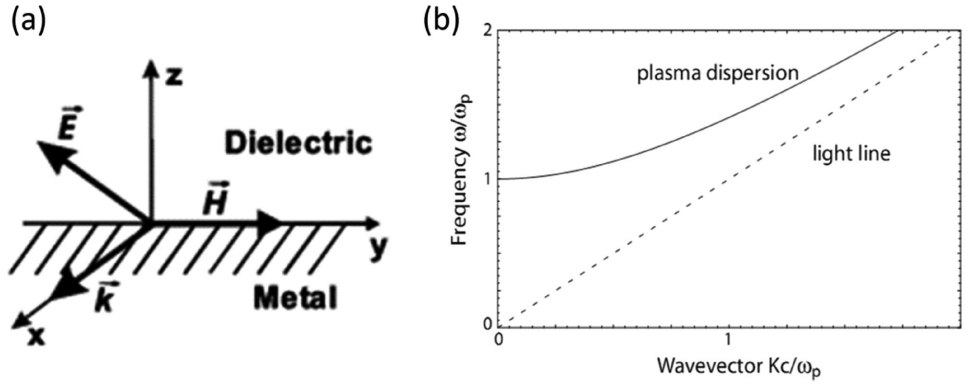

Figure 6. a) Spatial distribution of the magnetic intensity for a surface plasmon at the interface between gold and a dielectric in the direction perpendicular to the interface. b) The dispersion relation of the free electron gas. Electromagnetic wave propagation is only allowed for $\omega > \omega_p$. Reproduced with permission.[36] Copyright 2007, Springer.

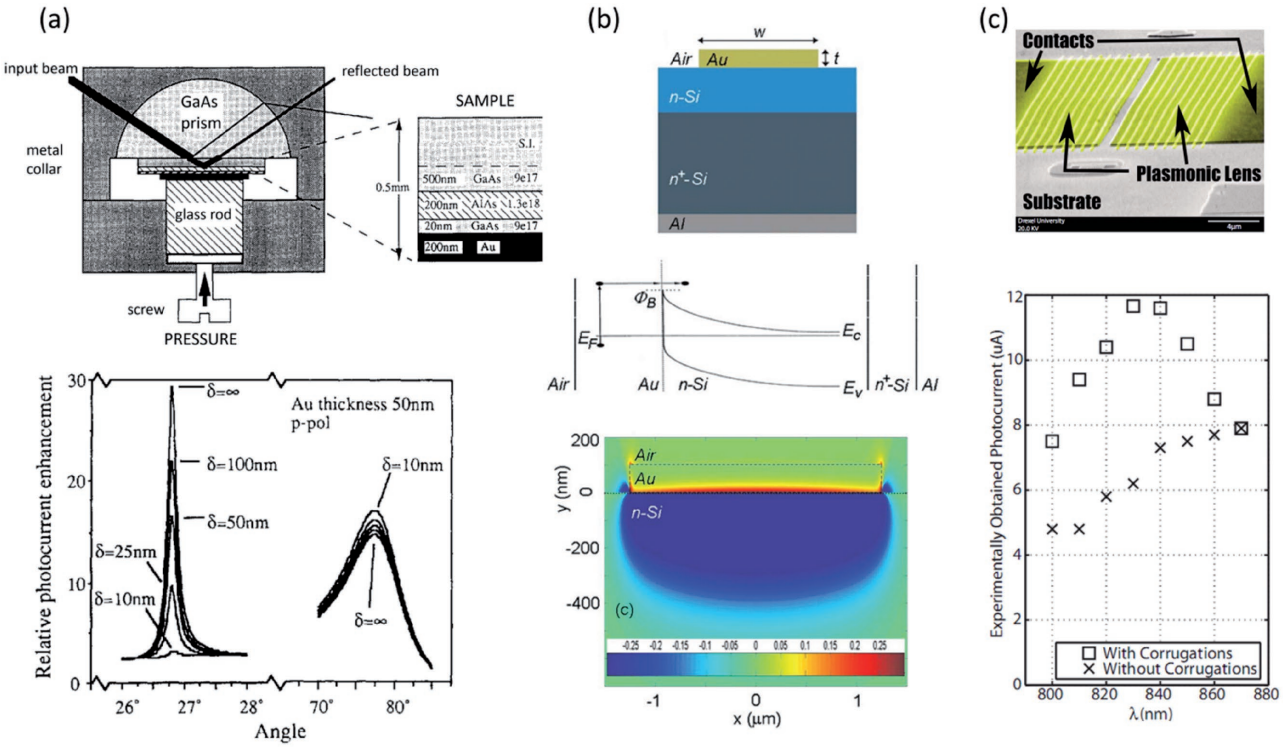

Figure 7. a) The experimental arrangement used to measure the reflectivity and photocurrent. The diagram on the left indicates how pressure was applied to ensure optical coupling between the prism and the sample. The diagram on the right shows a blown-up view of the sample indicating the thicknesses and doping of each layer (top). Relative photocurrent enhancement as a function of angle for p-polarized 1152 nm incident light. The two angular ranges show the enhancements due to surface plasmons being excited at the Au–air ($26 \leq 7 < 28°$) and GaAs–Au ($70° \leq 7 < 85°$3 interfaces (bottom). Reproduced with permission.[77] Copyright 1991, Elsevier. b) Front view of the photodetector structure on n-Si. The Au/n-Si interface serves simultaneously as part of the waveguide and as a Schottky barrier diode (top). Energy band diagram showing the internal photoemission process (middle). Perpendicular electric field distribution of the asb_b^0 mode (bottom). Reproduced with permission.[81] Copyright 2009, American Institute of Physics. c) Scanning electron microscope image of the planar integrated plasmonic lens MSM photodetector (top). Photocurrents of lensed and regular devices as a function of wavelength (bottom). Reproduced with permission.[85] Copyright 2009, American Institute of Physics.

in **Figure 7**a, a GaAs–A1As–GaAs–Au Schottky structure photodetector based on an Otto coupling geometry explored by Daboo et al. In this work, the incident p-polarized radiation could couple to the SPP at the Au–GaAs interface, and concentrate high *E*-fields arising from the excitation of SPPs at the GaAs–Au Schottky interface.[77] Thanks to a strong enhancement of the internal photoemission photocurrent across the Schottky barrier, an enhancement factor of 20 have been achieved.

SPP excited by an optical waveguide is developed from the bulk prism-based plasmonic devices. Unlike diffraction-limited dielectric waveguides, metallic waveguides can be fabricated at subwavelength dimensions. Benefitting from the same properties of optical signal transmission, they can be used for both optical and electrical signal transmission. Albeit the process of exciting SPPs in waveguide structure is similar to that of in attenuated total reflection prism coupler, photodetectors integrating with optical waveguides not only allows miniaturization of the photodetection system, but also provides a simple approach to control the optical path by the increased design constraints. As shown in Figure 7b, when the incident light is concentrated in the waveguiding layer, it evanescently penetrates through the metal layer. If the coupling condition for the guided mode and the surface plasmon is fulfilled as

$$\beta_{\text{mode}} = \text{Re}\{\beta_{\text{SP}}\} \tag{6}$$

where β_{mode} denotes the propagation constant of the waveguide mode. SPPs will be excited at the outer interface of the metal.[78]

Benefitting from the additional design waveguide integrated in devices, a variety of SPPs photodetectors in terms of fiber waveguide, symmetric/asymmetric metal strip waveguide, double metal strip waveguide based photodetectors with improved performance have been explored.[20,77,79–84] In order to better understand the effects of such SPPs waveguide structure in photodetection, a typical asymmetric structure waveguide Schottky Si photodetector would be demonstrated herein, because the asymmetric structure waveguide is the simplest structure among these devices. As shown in Figure 7b, this asymmetric structure waveguide Schottky Si photodetector is fabricated by thin Au stripes of finite width cladded with asymmetrical dielectric (lightly doped Si and air) to launch SPP.[81] By tailoring the thickness of Au strips, the coupling efficiency of 18% enhancement is achieved, and significant enhancement in quantum efficiency (the responsivity increases from 0.61 to 15.2 mA W^{-1}) is observed for a thin metal stripe due to multiple internal reflections of excited carriers. However, the performance of this kind of photodetector still need to be

improved compared with the symmetric metal stripe operating in the long-range SPPs. Because only a small portion of the incident light can be coupled into SPPs by end-fire excitation relying on spatial mode-matching rather than phase-matching, most of the incident light is reflected. Phase-matching to SPPs can be achieved in metal/dielectric multilayer thin film geometries such as insulator–metal–insulator (IMI) heterostructures sustain confined SPPs, this allows coupling SPP modes in conventional dielectric waveguides with high efficiency. In spite of these, there are three main techniques by which the missing momentum can be compensated up to now. First, making use of prism coupling to enhance the momentum of the incident light is a potential way. Second, a subwavelength protrusion or hole would provide a convenient way to generate SPPs locally. Third, making use of a periodic corrugation in the metal's surface is a promising method.[37] Because some techniques mentioned above involved the excitation and investigation of hybrid plasmons in metallic nanostructures, it will be presented in detail in Section 3.2.1.

Another approach to realize optical excitation of surface plasmons is based on the diffraction of light in a corrugated grating coupler. As illustrated in Figure 7c, the incident optical wave is diffracted and multipled to form a series of beams directed away from the surface at a variety of angles in this periodically distorted metal–dielectric interface. If the momentum of diffracted light parallel to the grating surface is equal to the propagation constant of the surface plasmon[78]

$$\frac{2\pi}{\lambda} n_{\mathrm{d}} \sin\theta + m\frac{2\pi}{\Lambda} = \pm \mathrm{Re}\{\beta^{\mathrm{SP}}\} \tag{7}$$

the diffracted light can couple to a surface plasmon, where m is an integer and denotes the diffraction order, Λ is the grating period. Benefiting from integrating a nanoscale metallic grating into its contacts, the photoelectric conversion efficiency of photodetectors is enhanced. As an example, Figure 7c is a MSM photodetector, in this photodetection system, SPPs are sensitive to the incidence angle, polarization, and wavelength of incident light through the equation as following[31,85]

$$K_x^{\mathrm{L}} + mk^{\mathrm{G}} = K_x^{\mathrm{SPP}} \tag{8}$$

where K_x^{L} is the x-directed component of K^{L}, m is an integer, and K_x^{SPP} is the SPP wave number. And the nanocorrugations play an important role for the additional momentum Δk required for the collective resonant coupling between incident photons and the electrons

$$k_{\parallel} = \frac{\omega}{c}\sin\theta \pm \Delta k = \frac{\omega}{c}\sqrt{\frac{\varepsilon_{\mathrm{d}}\varepsilon_{\mathrm{m}}}{\varepsilon_{\mathrm{d}}+\varepsilon_{\mathrm{m}}}} = k_{\mathrm{SP}} \tag{9}$$

where

$$\Delta k = \frac{2\pi l}{a}, l = 1, 2, 3, \tag{10}$$

where $k_{\parallel}$ is the component of the incident light wave vector parallel to the device surface, c is the speed of light, and θ is its angle of incidence, k_{SP} is the surface plasmon wave vector, and ε_{d} and ε_{m} are dielectric constants of air and metal, respectively. In this work, in addition to retain the MSM advantages of simplicity, planarity, and monolithic integrability, the integrated plasmonic lens photodetector with a high signal to noise ratio exhibits both a photocurrent enhancement and responsivity increase of about 90% at the design wavelength in comparison to other identical MSM photodetectors without integrated nanoscale gratings. Albeit with a drawback for such grating-based SPP photodetectors could only operate in a specified wavelength range, accurate control of the thickness of plasmonic active metal layer is not required in these devices, their compatibility with mass production makes the grating coupler an attractive approach for fabricating low cost SPP photodetectors.

3.2. Hybrid Plasmonic Photodetectors

In the plasmonic photodetectors, LSP mode, which provides large near-field enhancement factors and strong scattering, will gradually attenuate owing to losses arising from the absorption in the metallic materials. SPP mode is very conducive to guide and trap light into the active layer of photodetectors by compensating the missing momentum. Although the SPP mode could be used for light trapping, but the gains are modest because SPP waves only can be excited at specific angles and with one linear polarization state of incident light. Therefore, for the development of plasmon-enhanced photodetectors, activating SPP mode is very important for obtaining a high quantum efficiency. To cover the breadth of hybrid plasmonic photodetectors available at the present time with suitable classification, avenues will appear in these sections in terms of nanoantennas, hybrid gratings, and various microcavity architectures.

3.2.1. Plasmonic Photodetector Based on Optical Antenna

Followed by widely use of conventional radiowave antenna, optical antenna (nanoantenna) is a new intensively studied subject in physical optics. Albeit the working principle is quite different from classical antenna theory, the purpose of an optical antenna is similar to that of a conventional antenna: collect light over a broad space area and focus it on an ultrasmall area, and vice versa.[86] Up to now, various patterned metallic structures fabricated by electron-beam lithography with their minimum feature sizes in tens nanometers, which are the specific architectures allowed them to function as optical antennas. Hence, combined with the favorable attributes of LSPs and SPPs, optical antenna configurations possess a powerful capability of concentrating, manipulating, and controlling optical radiation at subwavelength scales. It means that if an appropriate optical antenna structure could be incorporated into a photodetector, surface plasmonic modes can be modified and transmitted over long distances, and the incident optical radiation would be converted into the nanoscale active region with a higher efficiency. In addition, similar to grating coupler-based SPR system mentioned above (Section 3.1.2), optical antenna can be integrated with photodetectors to generate hot electrons, which provides

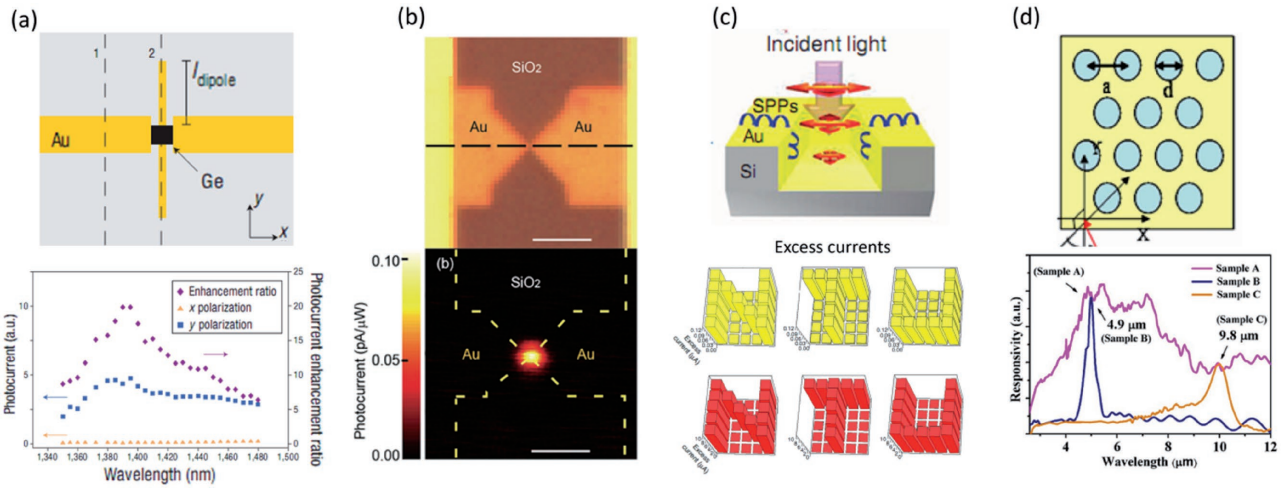

Figure 8. a) Top view of the open-sleeve dipole antenna consisting of a dipole antenna oriented in the *y* direction and two line electrodes (sleeves) in the *x* direction (top). Measured photocurrents for light polarization in *y* and *x* directions (bottom). Reproduced with permission.[87] Copyright 2011, American Chemical Society. b) Reflected light image of a typical device. The dashed line denotes the centerline of the Au electrodes (top). Photocurrent response at 780 nm as a function of laser position. Scale bar is 3 μm (bottom). Reproduced with permission.[22] Copyright 2008, Nature Publishing Group. c) DTTM active antenna structure on a Si-based device (top). Testing image constructed based on the existence or absence of a photocurrent during the point-by-point scanning of the DTTM device under low-intensity light at the wavelengths of 1310 (yellow) and 1550 (red) nm (bottom). Reproduced with permission.[23] Copyright 2014, Macmillan Publishers Limited. d) Hexagonal hole array of the quantum dot infrared photodetector (top), Infrared responsivities of the photodetectors with different periodic metal hole arrays (bottom). Reproduced with permission.[89] Copyright 2007, American Institute of Physics.

additional opportunities for photodetection at subwavelength region. Furthermore, the response peak of a photodetector could be selected by periodic optical antenna arrays owing to their extraordinary transmission properties. Therefore, scheme of fabricating nanostructure photodetector based on plasmonic antenna is quite fantastic. In this section, several representative nanoantenna architectures and important issues will be reviewed and discussed.

In several designs, dipole antenna is one of promising architecture to enhance the photocurrent of an ultrasmall photodetector with high wavelength and polarization selectivity. As an example depicted in **Figure 8**a, it is a subwavelength MSM detector equipped with a half-wave Hertz dipole antenna.[22] In this device, the resonant half-wave Hertz dipole antenna is made of two metallic nanowires, and the active region of this photodetector is 150 nm × 60 nm × 80 nm, which is two orders of magnitude smaller than previous photodetectors at such wavelengths in the range of 1310–1480 nm. In this device, owing to the dipole antenna, the incident light could be efficiently collected from a large area and concentrated into the small subwavelength region of the Ge, which allowed optical field and photocurrent to gain a great improvement with high polarization selectivity. As shown in Figure 8a (bottom), compared with the measured photocurrents for light polarization in *y* and *x* direction, a polarization contrast of 20 in the resulting photocurrent is found at a very low bias voltage. Additionally, the cutoff frequency of this device is estimated to be over 100 GHz, which suggests the photodetector possessing a great potential to operate with a high-speed. Therefore, although more precise techniques in the nanofabrication process are required, schemes of fabricating high performance nanostructure photodetectors assisted by optical antenna is indeed attractive.

Subsequently, thanks to the electron-beam lithography (EBL) and electromigration techniques, Shi et al. achieved a wavelength and polarization sensitive photodetector in individual sub 10 nm gold nanogap antenna in 2011.[87] As shown in Figure 8b, the device consists of a graphene constriction positioned within gap between two gold electrodes. Owing to the nanogap antenna, only a symmetric photocurrent is obtained at the narrowest region (≈10 nm) of the break junction device and the antisymmetric heating signal is suppressed when a Ti-sapphire tunable continuous wave laser scans along the dotted centerline of the electrodes. Moreover, polarization sensitivities of the photodetector could be achieved as large as 99%, and the largest photocurrent enhancement could be achieved around two orders of magnitudes. Subsequently, to further confirm the important role of nanogap antenna in the photodetection, the authors studied the photocurrents both on Au break junctions without graphene and graphene nanoconstrictions without nanogap gold electrodes, respectively. They found that the device without graphene do not produce any measurable photocurrent. And the device without nanogap Au electrodes only generate a antisymmetric heating-type signal which is independent of a resonant wavelength. This indeed confirms that the photocurrent enhancement originates from the coupling effect of Au nanogap electrode and graphene nanoconstriction. Therefore, this nanogap antenna holds promise for high performance detection at the nanoscale.

As mentioned above, benefiting from the focus ion beam (FIB) and electron beam lithography manufacturing processes, the size of optical antenna could be shrunken down to the nanoscale even sub-10 nm, In spite of this, photodetectors integrated with these optical antennas could operate with a high responsivity and broad bandwidth. Although photodetectors based on optical antenna are still at an early stage of

development, various optical antenna architectures were reported sequentially. Recently, in addition to planar antennas, a novel kind of photodetector based on a 3D cavity antenna fabricated by a conventional I-line lithography technique is proposed. As an "active" optical antenna, this deep-trench/thin-metal (DTTM) architecture (Figure 8c) can combine the functions of surface plasmon resonance, 3D cavity effects, and large-area Au/Si junctions within the same structure. And the responsivity is two orders of magnitude higher than those of LSP-based active nanoantennas with a broad bandwidth and polarization-insensitive. Moreover, as shown in Figure 8c, owing to the hot electrons could be generated and collected effectively in this architecture, the photocurrent reconstructed image of the letters "NTU" could be observed even at the wavelength of 1310 and 1550 nm, respectively. It demonstrated that, similar to surface-plasmon detector integrated with a metal waveguide (Section 3.1.1), this dual functional device could operate beyond the optical absorption regime of the Si material as well. Additionally, it is worth noting that the hole arrays with the same width and period as the DTTM structure were also studied in this work. Although the degree of near-field enhancement in these holes was much lower than that of in DTTM nanoantennas, sub-micrometer metal hole arrays can also act as the antenna to convert light into surface plasmons by providing the necessary momentum conservation for the coupling process. Besides that, sub-micrometer metal hole arrays exhibited extraordinary optical transmission phenomena with high electromagnetic fields in previous studies.[88] These fascinating features allowed them to integrate with a photodetector as a wavelength-tunable filter by tailoring the period and size of these holes.

Another interesting characteristic of optical antenna is wavelength selectivity. By controlling the geometric parameters of periodic metal hole arrays, extraordinary optical transmission could be obtained from the excitation of surface plasmons. As for this, Chang et al. proposed such a wavelength selective photodetectors in region of 3–5 and 8–12 μm, which are two transmission windows for electromagnetic radiation propagation in atmosphere. Briefly, it is a ten layer $In_{0.1}Ga_{0.9}As$/InAs/$In_{0.1}Ga_{0.9}As$/GaAs quantum dot infrared photodetector integrated with optical antenna like periodic Ag metal hole arrays (Figure 8d).[89] At first, the authors tailored the lattice constant and diameter of hexagonal ordered Ag hole arrays on the GaAs wafer to make the transmission peaks of spectra locate roughly at 5 and 9.9 μm, respectively. Subsequently, quantum dot infrared photodetectors without and with aforementioned periodic metal hole arrays were fabricated, respectively. Comparing with the responsivities of these samples (Figure 8d), it is not difficult to find that the response of pristine quantum dot infrared photodetector is broadband ranging from 2.5 to 12 μm (sample A), while the peak response of photodetectors with Ag metal hole arrays (sample B and sample C) are very narrow, and the operating wavelengths of the photodetector are consistent with that of aforementioned transmission spectra. Thus, it demonstrates that the wavelength selective photodetector could be modulated by the extraordinary transmission of metal arrays.

Apart from optical field enhancement and confinement by extraordinary absorption or transmission induced by plasmonic resonances, nanoantenna arrays can provide a phase shift and bend the path of light in unusual ways.[90,91] In addition, many other different optical antenna geometries have been studied, such as monopole antennas,[92,93] particle antennas,[94,95] cross antennas,[96,97] and patch antennas[98,99] and so forth, which provides us a plenty of powerful platforms for concentration and manipulation of light on small length scales.[86,100] Albeit studies of optical antennas are still in the initial stage most of them can only operate on a "light-in, light-out" basis, it is believed that the ability to convert optical radiation into photocurrent with a high-efficiency assisted by optical antennas would open additional opportunities for fabricating photodetectors with high performance or multifunctions.

3.2.2. Photodetectors Supported by Versatile Metallic Grating Waveguides

In previous section of Section 3.1.2, optical excitations of SPPs excited by grating or prism coupling were discussed. However, as for a standard grating construction, it usually launches SPPs from normally incident light in opposite directions simultaneously, and then only a small portion of the incident light can be coupled into SPPs, while most of incident light is reflected. Consequently, an important challenge for a standard grating construction is the coupling efficiency which is fundamentally limited. In spite of this, how to design a grating construction which could generate SPPs effectively with a controllable direction is another challenge. Therefore, to achieve high-efficiency excitation of SPPs from free-space beams, one should consider to explore novel grating structures for better mode-matching with the incident beam in terms of wavelength, angular range, and polarization. Fortunately, various hybrid metallic grating waveguides such as island-waveguide, dislocated double-layer metal gratings, double-grating-gate, resonant-cavity with double high-index-contrast grating mirrors, and metallic gratings coupled with photonic crystals have been proposed up to now. In the following sections, these promising photodetectors as well as potential building blocks will be discussed in detail.

To couple the incident light into the waveguide modes of detector efficiently, Stuart and Hall proposed an island-waveguide coupling configuration.[101] As shown in **Figure 9**a, this structure is composed of a metal island film, a thin absorbing layer, and an intermediate spacer layer. And the strength of interaction between islands and waveguide could be controlled by tailoring the thickness of intermediate spacer layer. Benefiting from this configuration, the incident light could be scattered with multiple internal reflections before escaping, and then a strong enhanced-absorption of the device is obtained. In addition, these metal islands can function as microscopic antennas, they could collect incident radiation and transfer the energy into nearby waveguide in all directions. Owing to the omnidirectional coupling, the waveguide modes of photodetector with copper islands gets a factor of twelve fold photocurrent enhancement in contrast to that of the pristine one. In addition to the metal island-waveguide, 1D metallic grating is an another strategy to generate SPPs for enhancing the light trapping. However, in this configuration, SPPs can be excited at specific angles and polarizations. It means that only less than 50%

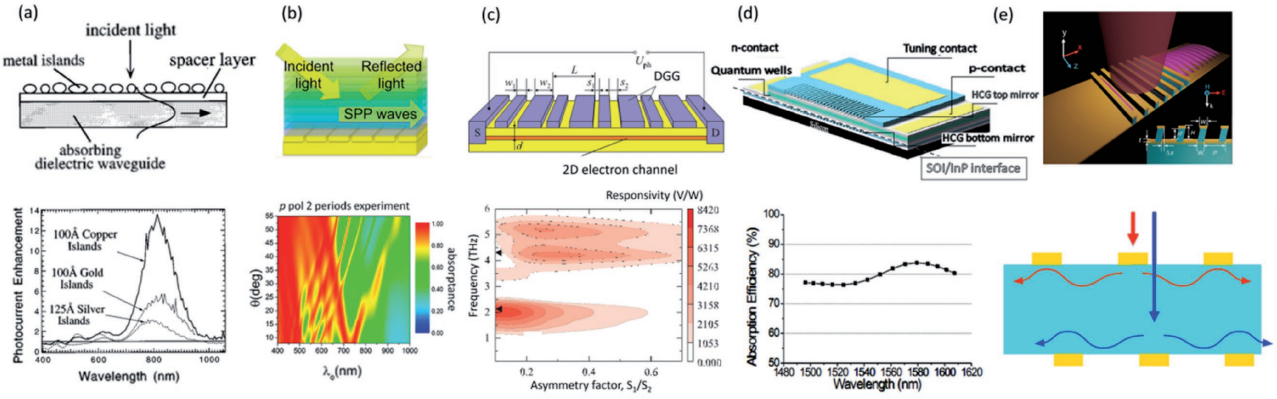

Figure 9. a) Island-waveguide coupling configuration (top). Measured the photocurrent of the device with the islands compared to that without the islands (bottom). Reproduced with permission.[101] Copyright1996, American Institute of Physics. b) Scheme illustration of 1D metallic grating coupled to a 1D photonic crystal (top). Density plots of absorptance as a function of θ and λ_o for incident p-polarized light obtained by theory and experiment (bottom). Reproduced with permission.[17] Copyright 2013, American Chemical Society. c) Plasmonic terahertz detection by a double-grating-gate field-effect transistor structure with an asymmetric unit (top). Calculated responsivity of the detector as a function of THz frequency and the asymmetry factor (bottom). Reproduced with permission.[19] Copyright 2011, American Institute of Physics. d) Cross-sectional profile of the proposed tunable resonant-cavity-enhanced photodetector with double high-index-contrast grating mirrors (top). Absorption efficiency as a function of wavelength (bottom). Reproduced with permission.[102] Copyright 2013, SPIE. e) Schematic of launching unidirectional SPP from normally incident beam by a dislocated double-layer metal grating. Inset is the geometric parameters of the structure (top). A schematic description of the interference model. Reproduced with permission.[18] Copyright 2014, American Chemical Society.

of unpolarized broadband light is available for this application. To address this problem, Hall et al. proposed that coupling a 1D metallic grating with a 1D photonic crystal instead of the homogeneous dielectric material was an effective way to decrease angular sensitivity[17] (Figure 9b). And their experimental results confirm that, benefiting from the additional 1D photonic crystal structure, the incident light could be trapped more efficiently. Because multiple SPPs can be activated by both incident p- and s-polarized light even when the wave vector of the incident light is wholly perpendicular to the grating lines. Hence, it suggests that this novel building block possesses tremendous potential for fabricating plasmonic photodetectors in near future.

To achieve a strong absorption and a competitive responsivity for a photodetector, a theoretical research demonstrates that an asymmetry double-grating gate is another candidate. In this configuration, the plasmon modes with both odd and even indexes could be excited well for terahertz detection.[19] Figure 9c gives a sketch of the strong asymmetry double-grating gate field-effect transistor. The double-grating gate is formed by two one-periodic coplanar metal subgratings, which are laterally shifted. And two successive slits between the fingers are of different widths. Because the asymmetry double-grating gate structure can function as an aerial matched antenna, the responsivity of this transistor could be achieved as high as 8 kV W^{-1}. This value is an order of magnitude greater than that of other uncooled plasmonic terahertz detectors.

In some cases, it is necessary to detect the light in a very narrow spectrum range. Thus, the ability to operate with high spectrum selectivity are essential for a photodetector. For this reason, Learkthanakhachon et al. proposed a novel resonant-cavity enhanced photodetector based on two high-index-contrast grating mirrors (Figure 9d).[102] Thanks to high reflectivity of two high-index-contrast gratings, the absorption of this photodetector is greatly enhanced only at wavelength of resonance in the optical cavity with a narrow linewidth smaller than 0.38 nm. These experimental results demonstrate that this hybrid grating-cavity structure is expected to be applied to design plasmonic photodetectors. And the details associated with photodetectors based on microcavity will be discussed in Section 3.2.3.

To take full advantage of the surface plasmon resonance energy in design a photodetector, launching surface plasmon polaritons in a desired direction may be an effective scheme to enhance the light absorption of the active area. As shown in Figure 9e, it is a novel dislocated double-layer metal grating structure which is composed of a slanted dielectric grating sandwiched and two gold gratings.[18] Due to the dislocation-induced constructively or destructively interference of the diffracted light from upper and lower gold gratings, the unidirectional coupling is achieved in this work. It is worth pointing out that, unlike the previous unidirectional couplers based on aperiodic structures, this coupler can be tailored flexibility by tuning the spacing and dislocation between two gratings. Therefore, this dislocated double-layer metal grating structure will provide an additional opportunity for fabricating a plasmonic photodetector with a high efficiency.

In brief, in spite of integrating plasmonic photodetectors with hybrid waveguides is still in its initial stages, many structures have been explored for fabricating photodetector. It is believed that taking advantage of their many attractive properties to excite coherent surface plasmon efficiently with low losses will lead to potentially fast, sensitive, and ultra-compact photodetectors.

3.2.3. Opportunities and Challenges for Microcavity-Based Plasmonic Photodetectors

In addition to nanoantenna and hybrid metallic grating waveguide mentioned above, fabricating photodetectors by using optical

microcavities is another alternative avenue to enhance the performance of device. By taking advantage of interference, diffraction or total reflection at the interface of two mediums, optical resonant cavity can transfer light energy from free space into desired small volumes by resonant recirculation. Incident light field can be confined in the cavity to increase the absorption efficiency of active layer. Hence, in conjunction with an appropriate resonant microcapacity on the photodetector is an appealing approach to increase the interaction length between incoming light and active materials. Up to now, some traditional optical microcavities such as Fabry–Pérot microcavity and whispering gallery cavity have been explored to enhance the photoelectric conversion efficiency of photodetectors with a high wavelength selectivity. However, it is still rather difficult to decrease the size of traditional optical microcavities down to subwavelength scale. Therefore, to further develop microcavity-based nanostructured photodetectors with high performance, a reinforcement of techniques is urgently needed. Fortunately, with the continuous development of micro–nanofabrication technology and semiconductor technique, photodetectors based on novel plasmonic resonant microcavities such as hybrid microcavities and photonic crystal defect cavities offer us a new possibility. In the following, the opportunities and challenges for these devices will be described.

As shown in **Figure 10**a, it is a typical Fabry–Pérot microcavity integrated with graphene photodetector.[27] By using the geometry design of Fabry–Pérot microcavity, more than 60% (for graphene without cavity, absorption coefficient is only 2.3%[103]) of the light is absorbed in the graphene, and the reflect spectral width $\Delta\lambda$ is only 9 nm at the cavity resonance wavelength. Hence, Fabry–Pérot microcavity causes a 26 fold absorption enhancement by confine the light wave inside the cavity, and 6.5 fold enhancement of electric field amplitude is obtained. Compared to a conventional bilayer graphene detector without cavity in the same geometrical dimensions, the responsivity of device with Fabry–Pérot microcavity is more than an order of magnitude stronger. Albeit the size of photodetectors proposed in this work is still too large to operate at subwavelength scale, Fabry–Pérot microcavity structure provide us an additional opportunity for fabricating plasmonic photodetectors with high photoelectric conversion efficiency and excellent wavelength selectivity.

Recently, Schmidt et al. developed a hybrid nanoparticle–microcavity-based plasmonic nanosensor.[25] As shown in Figure 10b, it is a nanoparticle–microcavity consisting of a single subwavelength metallic nanoparticle and a micrometer-thick film type cavity. In this hybrid system, Fabry–Pérot microcavity is formed of a high index thin film between low index substrate and air, which can be regarded as a wavelength filter or mode selector, and gold particles act as an optical antenna which can effectively concentrate the electromagnetic energy into the Fabry–Pérot microcavity. For the hybrid mode created by dipolar plasmonic resonance of single metallic nanoparticle and narrow bandwidth resonance of optical microcavity, the sensing figure-of-merit is boosted up to 36 times. Therefore, this kind of hybrid nanosensor combines the advantages of plasmonic nanoparticles with Fabry–Pérot microresonators, providing interesting features of incident-angle independent resonances, lateral ultrasmall sensing volume, and strongly improved detection resolution.

Aside from Fabry–Pérot microresonators, whispering gallery resonant microcavity is another candidate to store light of specific wavelengths. By continuous total internal reflection in circular orbits,[104] they possess the ability to enhance the absorption and responsivity of a photodetector. As an example, Figure 10c is an optical fiber sensor coupled with silica whispering gallery resonant cavities.[105] In this hybrid sensor, the photons can have more additional interaction time and probability of detection owing to the resonance microcavity structure.

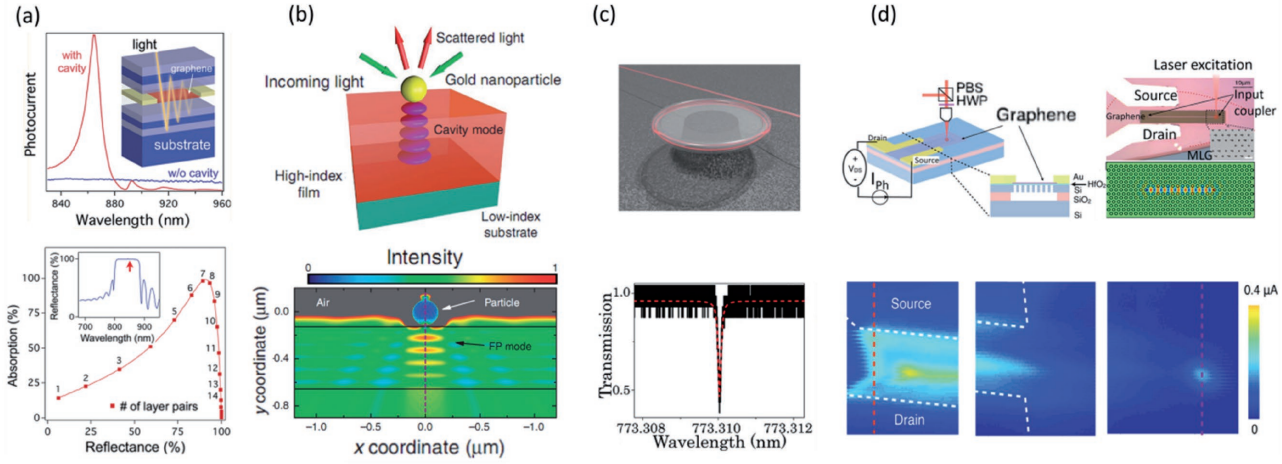

Figure 10. a) Fabry–Pérot microcavity-integrated graphene photodetector (top). Calculated dependence of optical absorption in a single-layer graphene sheet on the reflectivity of the top mirror. Inset: Measured reflectivity of the AlAs/$Al_{0.10}Ga_{0.90}As$ bottom mirror (bottom). Reproduced with permission.[27] Copyright 2012, American Chemical Society. b) Hybrid nanoparticle–microcavity-based plasmonic nanosensors, intensity distribution of a cross section of the particle-cavity system at an excitation wavelength of 616 nm (bottom). Spatial mapping of the photocurrent at the three areas. Reproduced with permission.[25] Copyright 1996, American Institute of Physics. c) Whispering-gallery microcavity sensors (top). Transmission spectrum for a quality factor measurement and Lorentzian fit (dashed red line). Reproduced with permission.[105] Copyright 1996, American Institute of Physics. d) Photonic crystal linear cavity integrated graphene photodetector. FDTD simulation of a localized resonant mode inside the PPC cavity (bottom). Reproduced with permission.[28] Copyright 2013, AIP Publishing.

Moreover, the resonant wavelength is determined by geometry sizes as well as device materials. Changes of these parameters will cause a detectable signal that can be used to determine the UV light exposure dose. From experimental measurement by scanning across a series of wavelength using tunable laser centered at 765 nm, resonant wavelength of the whispering gallery microcavity is determined to be 773.31 nm and the quality factor (Q) is extremely as high as 9 million. From the experimental results, the silica microcavity-based UV detector range with very linear performance in both forward and reverse directions, which demonstrates the reusability and reproducibility of the device. As a result of the inherently low nonlinear characteristic of silica, the device has a very high signal to noise ratio in ambient. Additionally, the response time of the microcavity integrated sensor is much faster than that of the polymer-coated fiber device, and the life time of microcavity integrated sensor is much longer. These indicate that the sensor based on optical fiber integrated with inorganic structure microcavity could operate with high performance.

Coincidentally, numerous micro–nano materials naturally possess whispering gallery microcavity structure, which makes the fabricating process more friendly and economically. Up to now, various novel whispering gallery microcavities based on microsphere,[106,107] microdisk,[108–110] microrod,[111,112] microcylinder,[113,114] microring/disk[115,116] have been explored. And they received considerable attention due to their appealing properties such as small volume, low-cost, and simple manufacturing processes and so forth. However, similar to the traditional Fabry–Pérot microcavity, the dimension of above mentioned whispering gallery microcavity is still as large as several tens of micrometers. Therefore, to obtain their nanoscale detection ability, it is believed that innovative approaches in conjunction with plasmonic technology are worthwhile to be further researched.

Unlike those two kinds of traditional microcavities mentioned above, photonic crystal defect microcavity is formed by dot defect or line defect in photonic crystal.[117–119] Therefore, it is one of the most promising architecture to shrink the size of plasmonic photodetectors down to the nanoscale up to now. Theoretically, when the intrinsic cavity loss rate k_c is equals to the loss rate into active material, k_{cm}, the cavity evanescent field strongly couples to the active material and enhancing the light–matter interaction in active material for generate photocurrent. As illustrated in Figure 10d, the planar photonic crystal (PPC) cavity integrated with graphene active layer is designed by Shiue et al.[28] Bounded cavity mode is produced by fabricating a linear defect in the center of PPC lattice. Finite-difference time-domain (FDTD) numerical simulation of the PPC cavity exhibits that the optical field is strongly localized in the line defect. A vertical cross-polarization confocal microscope with broad band excitation source (continue wavelength laser) is used to characterize the properties of PPC cavity.

Without graphene layer on top, multiple peaks between 1520 and 1550 nm correspond to the resonant modes within PPC cavity bandgap are found. However, due to the strongly coupling absorption of graphene, the peaks are lowered and broadened as graphene transfer on to the PPC cavity. For wavelength below 1550 nm, the input light is strongly enhanced in the line defect, which significantly increasing the absorption and the photocurrent in graphene. In addition, a spatial mapping of photocurrent shows that the photocurrent is mostly generated in the middle of the graphene channel, above the cavity line defect. Comparing with single pass graphene absorption, the absorption efficiency can reach as high as 95% by coupling the graphene with photonic crystal linear defect cavity, and the photocurrent is up to eight-fold enhancement.

In general, due to increase the interaction between incident light and active materials by resonance, photodetectors integrated with optical microcavities have shown significant enhancement in detection performances. In addition to the surface plasmon resonance, the resonant wavelength can also be tailored by the geometry of microcavities, such as length of Fabry-Pérot microcavity, the radius of whisper gallery microcavity, dimensions lattice and the defect of photonic crystal defect cavity. In spite of design and fabricating plasmonic resonant microcavities is still in its infancy, for the tendency of ultrasmall size integrated photodetector, applications of optical microcavity integrated in plasmonic photodetectors is promising.

4. Conclusions and Perspectives

It is no doubt that the merging of nanotechnology and optical technology will lead to remarkable development of surface plasmon resonance technology. Especially with getting deeper insights into the interaction between light and matter at nanoscale, versatile plasmonic nanostructures exhibit intriguing extraordinary absorption or transmission with a high direction and polarization controlled field enhancement and confinement. And many great achievements of plasmon integrated photodetectors are witnessed in the past few decades. Briefly, fabricating photodetectors in conjunction with plasmonic building blocks not only allows us to shrink device size down to the nanoscale without consideration of optical diffraction limit, but also provides us a powerful approach to enhance the photoelectric conversion efficiency at specific wavelength region without sacrificing speed and bandwidth.

In view of the basic scientific research and potential technological applications, advances in surface plasmon enhanced photodetectors as well as potential building blocks for fabricating plasmonic photodetectors are discussed herein. And these theory and experimental evidences demonstrate that plasmonic technique is indeed a promising pathway to fabricate nanostructured photodetector with desirable capabilities. However, studies on this field are still in infancy up to now, and many important issues are waiting for solving. Of course, every challenge is an opportunity. Therefore, for the further development of plasmonic photodetectors in the future, the following aspects may be become the focuses. First, the primary problem is that how to design and fabricate a plasmonic photodetector with a high resonance field enhancement and a low metal absorption loss. Therefore, the shape, size and surrounding dielectric medium of metallic nanoparticle placed on or close to the active region of a photodetector should be carefully considered. In spite of this, to avoid the issues of metal absorption loss, exploring other kind of materials such as graphene or heavy doping semiconductor function as a plasmonic

building block in a photodetector is promising.[120–127] Furthermore, because of the resonant plasmon field enhancement can also be modified by geometry of optical component, make efforts to integrate photodetector with hybrid optical antenna, waveguide, and microcavity is an alternative approach to figure out this puzzle. Second, according to the energy match principle, most of surface plasmon enhanced photodetectors can only work in the visible or IR range up to now, it is means that another challenge is exploring a high direction, polarization controlled plasmon integrated photodetector at the short wavelength region. To overcome this tough issue, getting insight in the mechanism of coupling interaction among metal nanoparticles and design appropriate plasmonic clusters such as Fano-resonant plasmonic clusters may be a possible solution.[128–134] Third, how to bring these type of photodetectors out of lab to an industrial fabrication is worth looking forward to. Benefiting from FIB or EBL manufacturing processes, dimensions of the plasmon nanostructure could be accurately controlled in the range from tens to hundreds nanometer which has already led researchers to explore the underlying science and design a more reasonable device structure. However, both of them are complicated and expensive. Therefore, exploitation of a new nanofabrication technique with low costs and scalable-production is essential to the further development of these photodetectors.

In summary, as a new class of subwavelength photonic devices, surface plasmons with many amazing properties show great potential for fabricating nanostructure photodetectors with desirable abilities. Nowadays, there is still plenty of room to be taken full advantage of this technology. It is believed that with deeper understanding of their intrinsic physical mechanisms via further development of nanofabrication technologies, plasmonic photodetectors will possess a bright future in this industry 4.0 era.

Acknowledgements

H.Y.C., L.X.S, and M.M.J contributed equally to this work. The authors would like to thank Ruidie Tang for her kind help. This work was supported by the National Natural Science Foundation of China (Grant Nos. 61505033, 61528402, 11674061, 51471051, 11404328, 61705043 and 11574307), National Postdoctoral Science Foundation of China (2017M611441), Science and Technology Commission of Shanghai Municipality (15520720700), and Shanghai Shu Guang Project (12SG01). Key Laboratory of Micro-systems and Micro-structures Manufacturing of Ministry of Education, Harbin Institute of Technology (2017KM003).

Conflict of Interest

The authors declare no conflict of interest.

Keywords

nanostructures, photodetectors, superintegration, surface plasmon resonances

Received: July 25, 2017
Revised: August 15, 2017
Published online: October 10, 2017

[1] D. Culler, D. Estrin, M. Srivastava, *Computer* **2004**, *37*, 41.
[2] H. Chen, H. Liu, Z. Zhang, K. Hu, X. S. Fang, *Adv. Mater.* **2016**, *28*, 403.
[3] V. J. Sorger, R. F. Oulton, R. Ma, X. Zhang, *MRS Bull.* **2012**, *37*, 728.
[4] E. Monroy, F. Omnès, F. Calle, *Semicond. Sci. Technol.* **2003**, *18*, R33.
[5] X. S. Fang, L. F. Hu, K. F. Huo, B. Gao, L. J. Zhao, M. Y. Liao, P. K. Chu, Y. Bando, D. Golberg, *Adv. Funct. Mater.* **2011**, *21*, 3907.
[6] S. Kang, S. C. Lee, S. H. Lee, K. Y. Lee, J. J. Jeong, Y. S. Lee, K. Nam, H. S. Chang, W. Y. Chung, C. S. Park, *Surgery* **2009**, *146*, 1048.
[7] F. Schwierz, *Nat. Nanotechnol.* **2010**, *5*, 487.
[8] https://www03.ibm.com/press/us/en/pressrelease/47301, September 2015.
[9] J. A. Schuller, E. S. Barnard, W. Cai, Y. C. Jun, J. S. White, *Nat. Mater.* **2010**, *9*, 193.
[10] E. Ozbay, *Science* **2006**, *311*, 189.
[11] V. E. Ferry, L. A. Sweatlock, D. Pacifici, H. A. Atwater, *Nano Lett.* **2008**, *8*, 4391.
[12] K. Okamoto, I. Niki, A. Shvartser, Y. Narukawa, T. Mukai, *Nat. Mater.* **2004**, *3*, 601.
[13] G. Konstantatos, E. H. Sargent, *Nat. Nanotechnol.* **2010**, *5*, 391.
[14] K. Hu, H. Chen, M. Jiang, F. Teng, L. Zheng, X. S. Fang, *Adv. Funct. Mater.* **2016**, *26*, 6641.
[15] W. Zhang, J. Xu, W. Ye, Y. Li, Z. Qi, J. Dai, Z. Wu, C. Chen, J. Yin, J. Li, H. Jiang, Y. Fang, *Appl. Phys. Lett.* **2015**, *106*, 21112.
[16] H. R. Stuart, D. G. Hall, *Appl. Phys. Lett.* **1998**, *73*, 3815.
[17] A. S. Hall, M. Faryad, G. D. Barber, L. Liu, S. Erten, T. S. Mayer, A. Lakhtakia, T. E. Mallouk, *ACS Nano* **2013**, *7*, 4995.
[18] T. Liu, Y. Shen, W. Shin, Q. Zhu, S. Fan, C. Jin, *Nano Lett.* **2014**, *14*, 3848.
[19] V. V. Popov, D. V. Fateev, T. Otsuji, Y. M. Meziani, D. Coquillat, *Appl. Phys. Lett.* **2011**, *199*, 243504.
[20] X. Wang, Z. Cheng, K. Xu, H. K. Tsang, J. B. Xu, *Nat. Photonics* **2013**, *7*, 888.
[21] S. I. Bozhevolnyi, V. S. Volkov, E. Devaux, J. Laluet, T. W. Ebbesen, *Nature* **2006**, *440*, 508.
[22] T. Liang, S. E. Kocabas, S. Latif, A. K. Okyay, D. S. Lygagnon, *Nat. Photonics* **2008**, *2*, 226.
[23] K. T. Lin, H. L. Chen, Y. S. Lai, C. C. Yu, *Nat. Commun.* **2014**, *5*, 3288.
[24] Q. Li, Z. Li, N. Li, X. Chen, P. Chen, X. Shen, W. Lu, *Sci. Rep.* **2014**, *4*, 6332.
[25] M. A. Schmidt, D. Y. Lei, L. Wondraczek, V. Nazabal, S. A. Maier, *Nat. Commun.* **2012**, *3*, 1108.
[26] M. Engel, M. Steiner, A. Lombardo, A. C. Ferrari, H. V. Lohneysen, P. Avouris, R. Krupke, *Nat. Commun.* **2012**, *3*, 906.
[27] M. Furchi, A. Urich, A. Pospischil, G. Lilley, K. Unterrainer, H. Detz, P. Klang, A. M. Andrews, W. Schrenk, G. Strasser, T. Mueller, *Nano Lett.* **2012**, *12*, 2773.
[28] R. Shiue, X. Gan, Y. Gao, L. Li, X. Yao, A. Szep, D. Walker Jr., J. Hone, D. Englund, *Appl. Phys. Lett.* **2013**, *103*, 241109.
[29] H. A. Atwater, A. Polman, *Nat. Mater.* **2010**, *9*, 205.
[30] R. Zia, J. A. Schuller, A. Chandran, M. L. Brongersma, *Mater. Today* **2006**, *9*, 20.
[31] P. Berini, *Laser Photonics Rev.* **2014**, *8*, 197.
[32] J. Homola, S. S. Yee, G. Gauglitz, *Sens. Actuators B* **1999**, *54*, 3.
[33] R. Manijeh, A. Rogalski, *J. Appl. Phys.* **1996**, *79*, 7433.
[34] K. Liu, M. Sakurai, M. Aono, *Sensors* **2010**, *10*, 8604.
[35] G. Armelles, A. Cebollada, A. García-Martín, M. U. González, *Adv. Opt. Mater.* **2013**, *1*, 10.
[36] S. A. Maier, *Plasmonics: Fundamentals and Application*, Springer, New York **2007**.
[37] W. L. Barnes, A. Dereux, T. W. Ebbesen, *Nature* **2003**, *424*, 824.
[38] X. Liu, Y. Feng, K. Chen, B. Zhu, J. Zhao, T. Jiang, *Opt. Express* **2014**, *22*, 20107.

[39] Y. Yao, R. Shankar, P. Rauter, Y. Song, J. Kong, M. Loncar, F. Capasso, *Nano Lett.* **2014**, *14*, 3749.
[40] S. M. Sze, K. K. Ng, *Physics of Semiconductor Devices*, John Wiley & Sons, Hoboken, NJ, USA **2006**.
[41] H. Chen, K. Liu, L. Hu, A. A. Al-Ghamdi, X. Fang, *Mat. Today* **2015**, *18*, 493.
[42] M. L. Brongersma, N. J. Halas, P. Nordlander, *Nat. Nanotechnol.* **2015**, *10*, 25.
[43] C. Clavero, *Nat. Photonics* **2014**, *8*, 95.
[44] P. Neutens, P. van Dorpe, *Active Plasmonics and Tuneable Plasmonic Metamaterials*, John Wiley & Sons, Inc., Hoboken, NJ, USA **2013**, p. 219.
[45] T. Mokari, C. G. Sztrum, A. Salant, E. Rabani, U. Banin, *Nat. Mater.* **2005**, *4*, 855.
[46] M. Chen, L. Shao, S. V. Kershaw, H. Yu, J. Wang, A. L. Rogach, N. Zhao, *ACS Nano* **2014**, *8*, 8208.
[47] E. Prodan, C. Radloff, N. J. Halas, P. Nordlander, *Science* **2003**, *302*, 419.
[48] J. Zhu, J. Li, J. Zhao, *Plasmonics* **2011**, *6*, 527.
[49] P. Nordlander, *ACS Nano* **2009**, *3*, 488.
[50] F. Hao, P. Nordlander, Y. Sonnefraud, P. V. Dorpe, S. A. Maier, *ACS Nano* **2009**, *3*, 643.
[51] Y. H. Fu, J. B. Zhang, Y. F. Yu, B. Luk'Yanchuk, *ACS Nano* **2012**, *6*, 5130.
[52] L. J. Sherry, S. Chang, G. C. Schatz, R. P. Van Duyne, B. J. Wiley, Y. Xia, *Nano Lett.* **2005**, *5*, 2034.
[53] Y. Xiong, B. Wiley, J. Chen, Z. Y. Li, Y. Yin, Y. Xia, *Angew. Chem.* **2005**, *44*, 7913.
[54] J. Chen, Z. Li, S. Yue, J. Xiao, Q. Gong, *Nano Lett.* **2012**, *12*, 2494.
[55] E. Hendry, F. J. Garcia-Vidal, L. Martin-Moreno, J. G. Rivas, M. Bonn, A. P. Hibbins, M. J. Lockyear, *Phys. Rev. Lett.* **2008**, *100*, 123901.
[56] H. F. Ghaemi, T. Thio, D. E. Grupp, T. W. Ebbesen, H. J. Lezec, *Phys. Rev. B* **1998**, *58*, 6779.
[57] C. Genet, M. P. van Exter, J. P. Woerdman, *Opt. Commun.* **2003**, *225*, 331.
[58] V. W. Brar, M. S. Jang, M. Sherrott, S. Kim, J. J. Lopez, L. B. Kim, M. Choi, H. Atwater, *Nano Lett.* **2014**, *14*, 3876.
[59] Y. Li, H. Yan, D. B. Farmer, X. Meng, W. Zhu, R. M. Osgood, T. F. Heinz, P. Avouris, *Nano Lett.* **2014**, *14*, 1573.
[60] S. Alkis, F. B. Oru, B. Orta, A. K. Ger, A. K. Okyay, *J. Opt.* **2012**, *14*, 125001.
[61] L. B. Luo, L. H. Zeng, C. Xie, Y. Q. Yu, F. X. Liang, C. Y. Wu, L. Wang, J. G. Hu, *Sci. Rep.* **2014**, *4*, 3914.
[62] P. Senanayake, C. H. Hung, J. Shapiro, A. Lin, B. Liang, *Nano Lett.* **2011**, *11*, 5279.
[63] C. Noguez, *J. Phys. Chem. C* **2007**, *111*, 3806.
[64] B. Luk'Yanchuk, N. I. Zheludev, S. A. Maier, N. J. Halas, P. Nordlander, H. Giessen, C. T. Chong, *Nat. Mater.* **2010**, *9*, 707.
[65] R. N. Stuart, F. Wooten, W. E. Spicer, *Phys. Rev. Lett.* **1963**, *10*, 7.
[66] G. Bao, D. Li, X. Sun, M. Jiang, Z. Li, H. Song, H. Jiang, Y. Chen, G. Miao, Z. Zhang, *Opt. Express* **2014**, *22*, 24286.
[67] K. Liu, M. Sakurai, M. Liao, M. Aono, *J. Phys. Chem. C.* **2010**, *114*, 19835.
[68] D. Li, X. Sun, H. Song, Z. Li, Y. Chen, H. Jiang, G. Miao, *Adv. Mater.* **2012**, *24*, 845.
[69] H. Hsiao, I. Ni, S. Tzeng, W. Lin, C. Lin, *Nanoscale Res. Lett.* **2014**, *9*, 640.
[70] X. Wang, K. Liu, X. Chen, B. Li, M. Jiang, Z. Zhang, H. Zhao, D. Shen, *ACS Appl. Mater. Int.* **2017**, *9*, 5574.
[71] M. Sun, Z. Xu, M. Yin, Q. Lin, L. Lu, X. Xue, X. Zhu, Y. Cui, Z. Fan, Y. Ding, *Nanoscale* **2016**, *8*, 8924.
[72] V. E. Ferry, M. A. Verschuuren, H. B. Li, E. Verhagen, R. J. Walters, R. E. Schropp, H. A. Atwater, A. Polman, *Opt. Express* **2010**, *18*, A237.
[73] V. E. Ferry, L. A. Sweatlock, D. Pacifici, H. A. Atwater, *Nano Lett.* **2008**, *8*, 4391.
[74] J. Wu, F. Chen, Y. Hsiao, F. Chien, P. Chen, C. Kuo, M. H. Huang, C. Hsu, *ACS Nano* **2011**, *5*, 959.
[75] J. L. Hou, A. Fischer, S. C. Yang, J. Benduhn, J. Widmer, D. Kasemann, K. Vandewal, K. Leo, *Adv. Funct. Mater.* **2016**, *26*, 5741.
[76] J. Homola, S. S. Yee, G. Gauglitz, *Sens. Actuators* **1999**, *54*, 3.
[77] C. Daboo, M. J. Baird, H. P. Hughes, N. Apsley, M. T. Emeny, *Thin Solid Films* **1991**, *201*, 9.
[78] J. Homola, *Chem. Rev.* **2008**, *108*, 462.
[79] T. Yin, R. Cohen, M. M. Morse, G. Sarid, Y. Chetrit, D. Rubin, M. J. Paniccia, *Opt. Express* **2007**, *15*, 13965.
[80] N. Youngblood, Y. Anugrah, R. Ma, S. J. Koester, M. Li, *Nano Lett.* **2014**, *14*, 2741.
[81] A. Akbari, P. Berini, *Appl. Phys. Lett.* **2009**, *95*, 21104.
[82] F. Ren, K. Ang, J. Song, Q. Fang, M. Yu, G. Lo, D. Kwong, *Appl. Phys. Lett.* **2010**, *97*, 91102.
[83] C. Scales, P. Berini, *IEEE J. Quantum Electron.* **2010**, *46*, 633.
[84] N. Youngblood, C. Chen, S. J. Koester, M. Li, *Nat. Photonics* **2015**, *9*, 247.
[85] J. A. Shackleford, R. Grote, M. Currie, J. E. Spanier, B. Nabet, *Appl. Phys. Lett.* **2009**, *94*, 83501.
[86] L. Novotny, N. van Hulst, *Nat. Photonics* **2011**, *5*, 83.
[87] S. Shi, X. Xu, D. C. Ralph, P. L. McEuen, *Nano Lett.* **2011**, *11*, 1814.
[88] C. Genet, T. W. Ebbesen, *Nature* **2007**, *445*, 39.
[89] C. Chang, H. Chang, C. Chen, M. Tsai, Y. Chang, S. Lee, S. Tang, *Appl. Phys. Lett.* **2007**, *91*, 163107.
[90] X. Ni, N. K. Emani, A. V. Kildishev, A. Boltasseva, V. M. Shalaev, *Science* **2012**, *335*, 427.
[91] N. Engheta, *Science* **2011**, *334*, 317.
[92] T. H. Taminiau, F. D. Stefani, F. B. Segerink, N. F. Van Hulst, *Nat. Photonics* **2008**, *2*, 234.
[93] T. H. Taminiau, R. J. Moerland, F. B. Segerink, L. Kuipers, N. F. van Hulst, *Nano Lett.* **2007**, *7*, 28.
[94] P. Anger, P. Bharadwaj, L. Novotny, *Phys. Rev. Lett.* **2006**, *96*, 113002.
[95] E. S. Ünlü, R. U. Tok, K. Şendur, *Opt. Express* **2011**, *19*, 1000.
[96] H. Iwasaki, *IEEE Trans. Antennas Propag.* **1996**, *44*, 1399.
[97] L. V. Brown, K. Zhao, N. King, H. Sobhani, P. Nordlander, N. J. Halas, *J. Am. Chem. Soc.* **2013**, *135*, 3688.
[98] F. Yang, X. Zhang, X. Ye, Y. Rahmat-Samii, *IEEE Trans. Antennas Propag.* **2001**, *49*, 1094.
[99] S. Maci, G. B. Gentili, *IEEE Antennas Propag. Mag.* **1997**, *39*, 13.
[100] P. Muhlschlegel, *Science* **2005**, *308*, 1607.
[101] H. R. Stuart, D. G. Hall, *Appl. Phys. Lett.* **1996**, *69*, 2327.
[102] S. Learkthanakhachon, K. Yvind, I. Chung, presented at *SPIE Photonics West: High Contrast Metastructures II*, San Francisco, California, United States **2013**.
[103] A. N. Grigorenko, M. Polini, K. S. Novoselov, *Nat. Photonics* **2012**, *6*, 749.
[104] K. J. Vahala, *Nature* **2003**, *424*, 839.
[105] A. Harker, S. Mehrabani, A. M. Armani, *Opt. Lett.* **2013**, *38*, 3422.
[106] M. Larsson, K. N. Dinyari, H. Wang, *Nano Lett.* **2009**, *9*, 1447.
[107] X. Fan, P. Palinginis, S. Lacey, H. Wang, M. C. Lonergan, *Opt. Lett.* **2000**, *25*, 1600.
[108] E. Peter, P. Senellart, D. Martrou, A. Lemaître, J. Hours, J. M. Gérard, J. Bloch, *Phys. Rev. Lett.* **2005**, *95*, 67401.
[109] S. L. McCall, A. Levi, R. E. Slusher, S. J. Pearton, R. A. Logan, *Appl. Phys. Lett.* **1992**, *60*, 289.
[110] B. Min, E. Ostby, V. Sorger, E. Ulin-Avila, L. Yang, X. Zhang, K. Vahala, *Nature* **2009**, *457*, 455.

[111] L. Sun, Z. Chen, Q. Ren, K. Yu, L. Bai, W. Zhou, H. Xiong, Z. Q. Zhu, X. Shen, *Phys. Rev. Lett.* **2008**, *100*, 156403.
[112] M. Kazes, D. Y. Lewis, U. Banin, *Adv. Funct. Mater.* **2004**, *14*, 957.
[113] X. Yi, Y. Xiao, Y. Li, Y. Liu, B. Li, Z. Liu, Q. Gong, *Appl. Phys. Lett.* **2010**, *97*, 203705.
[114] M. A. Kaliteevski, S. Brand, R. A. Abram, A. Kavokin, L. S. Dang, *Phys. Rev. B* **2007**, *75*, 233309.
[115] D. Rafizadeh, J. P. Zhang, S. C. Hagness, A. Taflove, K. A. Stair, S. T. Ho, R. C. Tiberio, *Opt. Lett.* **1997**, *22*, 1244.
[116] D. Rafizadeh, J. P. Zhang, R. C. Tiberio, S. T. Ho, *J. Lightwave Technol.* **1998**, *16*, 1308.
[117] O. Painter, R. K. Lee, A. Scherer, A. Yariv, J. D. O'Brien, P. D. Dapkus, I. Kim, *Science* **1999**, *284*, 1819.
[118] M. Qi, E. Lidorikis, P. T. Rakich, S. G. Johnson, J. D. Joannopoulos, E. P. Ippen, H. I. Smith, *Nature* **2004**, *429*, 538.
[119] T. D. Happ, I. I. Tartakovskii, V. D. Kulakovskii, J. Reithmaier, M. Kamp, A. Forchel, *Phys. Rev. B* **2002**, *66*, 41303.
[120] D. C. Look, K. D. Leedy, D. B. Thomson, B. Wang, *J. Appl. Phys.* **2014**, *115*, 12002.
[121] G. V. Naik, J. Liu, A. V. Kildishev, V. M. Shalaev, A. Boltasseva, *Proc. Natl. Acad. Sci. USA* **2012**, *109*, 8834.
[122] A. N. Grigorenko, M. Polini, K. S. Novoselov, *Nat. Photonics* **2012**, *6*, 749.
[123] F. J. Garcia De Abajo, *ACS Photonics* **2014**, *1*, 135.
[124] T. J. Echtermeyer, L. Britnell, P. K. Jasnos, A. Lombardo, R. V. Gorbachev, A. N. Grigorenko, A. K. Geim, A. C. Ferrari, K. S. Novoselov, *Nat. Commun.* **2011**, *2*, 458.
[125] S. Kalusniak, S. Sadofev, F. Henneberger, *Phys. Rev. Lett.* **2014**, *112*, 137401.
[126] D. C. Look, K. D. Leedy, *Appl. Phys. Lett.* **2013**, *102*, 182107.
[127] P. R. West, S. Ishii, G. V. Naik, N. K. Emani, V. M. Shalaev, A. Boltasseva, *Laser Photonics Rev.* **2010**, *4*, 795.
[128] B. J. Lawrie, K. Kim, D. P. Norton, R. F. Haglund Jr., *Nano Lett.* **2012**, *12*, 6152.
[129] S. Fan, W. Suh, J. D. Joannopoulos, *JOSA A* **2003**, *20*, 569.
[130] B. Luk'Yanchuk, N. I. Zheludev, S. A. Maier, N. J. Halas, P. Nordlander, H. Giessen, C. T. Chong, *Nat. Mater.* **2010**, *9*, 707.
[131] H. Chen, K. Liu, M. Jiang, Z. Zhang, L. Liu, B. Li, X. Xie, F. Wang, D. Zhao, C. Shan, D. Shen, *J. Phys. Chem. C.* **2014**, *118*, 679.
[132] N. J. Halas, S. Lal, S. Link, W. S. Chang, D. Natelson, J. H. Hafner, P. Nordlander, *Adv. Mater.* **2012**, *24*, 4842.
[133] Z. Yang, Z. Zhang, L. Zhang, Q. Li, Z. Hao, Q. Wang, *Opt. Lett.* **2011**, *36*, 1542.
[134] H. Chen, K. Liu, M. Jiang, Z. Zhang, X. Xie, D. Wang, L. Liu, B. Li, D. Zhao, C. Shan, *Appl. Phys. Lett.* **2014**, *104*, 91119.

